Energy band dispersion in photoemission spectra of argon clusters

Marko Förstel[1,2], Melanie Mucke[1], Tiberiu Arion[1], Toralf Lischke[1,⊕], Silko Barth[1], Volker Ulrich[1], Gunnar Öhrwall[3,*], Olle Björneholm[3], Uwe Hergenhahn[1,+] and Alex M. Bradshaw[1,4]

[1]*Max-Planck-Institut für Plasmaphysik (IPP), EURATOM Association, Boltzmannstr. 2, 85748 Garching, Germany*

[2]*Max-Planck-Institut für Kernphysik, Saupfercheckweg 1, 69117 Heidelberg, Germany*

[3]*Division of Molecular and Condensed Matter Physics, Department of Physics and Astronomy, Box 516, Uppsala University, SE-75120 Uppsala, Sweden*

[4]*Fritz-Haber-Institut der Max-Planck-Gesellschaft, Faradayweg 4- 6, 14195 Berlin, Germany*

Using photoemission we have investigated free argon clusters from a supersonic nozzle expansion in the photon energy range from threshold up to 28 eV. Measurements were performed both at high resolution with a hemispherical electrostatic energy analyser and at lower resolution with a magnetic bottle device. The latter experiments were performed for various mean cluster sizes. In addition to the ≈ 1.5 eV broad 3p-derived valence band seen in previous work, there is a sharper feature at ≈ 15 eV binding energy. Surprisingly for non-oriented clusters, this peak shifts smoothly in binding energy over the narrow photon energy range 15.5 – 17.7 eV, indicating energy band dispersion. The onset of this bulk band-like behaviour could be determined from the cluster size dependence.

Keywords: Cluster; Band Structure; Argon; Photoelecton Spectroscopy.

PACS numbers: 36.40.Cg, 61.46.Bc, 71.20.Ps

1. Introduction

One of the main reasons for investigating small particles of matter, often termed "clusters", is to establish when - as a function of increasing size - a change from molecular-like to bulk-like behaviour takes place. The weakly bound, so-called van der Waals clusters formed by the rare gases are model systems on which to investigate this phenomenon. The fluorescence spectra of Möller and co-workers have shown that the intensity ratio of surface to volume excitons in krypton [1] and argon [2] clusters changes as a function of mean cluster size. In Kr clusters bulk excitons start to appear above $\langle N \rangle = 200$. Similarly, recent high-resolution core and valence photoelectron studies of rare-gas clusters have allowed surface and bulk contributions to the spectra to be distinguished [3-9]. On the basis of the width of the 5p valence band and the ratio of the surface to bulk contribution as a function of Xe cluster size, Rolles et al. [7, 8] conclude that bulk-like electronic band formation occurs for a mean size $\langle N \rangle$ above 500 (as determined by so-called scaling laws [10]). It would be useful to replace this rather indirect estimation of the onset of bulk band-like behaviour by a more quantitative approach.

An important signature of bulk electronic properties is the observation of the dispersion of energy bands in a photoemission experiment, provided that the system shows sufficient long-range order. In such an experiment on an oriented bulk single crystal dispersion manifests itself as a photon energy-dependent or emission angle-dependent shift of the photoemission peak caused by an optical transition in which crystal momentum is conserved. These are the well-known vertical transitions in the conventional, reduced zone representation of the three-dimensional electronic band structure (e.g. Ref [11]). Photoemission experiments on both polycrystalline argon films by Schwentner et al [12] and, more recently, on (111)-oriented argon single crystals by Kassühlke et al [13] show strong dispersion effects at photon energies just above threshold. In the present paper we report 3p valence band photoemission data for argon clusters of different mean sizes. In general, the spectra agree with those reported in previous work of Feifel et al. [5], Rolles et al [7, 8] and Hergenhahn et al [9], except for the observation of a relatively sharp feature at a binding energy of ca. 15 eV, which also shows dispersion. The results are compared with previous solid state studies and the implications of the cluster size dependence discussed. A preliminary account of this work has appeared in Ref. [14].

2. Experimental

Photoelectron spectra of free Ar clusters were measured at the third generation synchrotron radiation source BESSY II on the recently constructed UE112/lowE PGMa beamline [15]. Horizontally linearly polarized radiation was used. The apparatus for production of the cluster jet and for recording the photoelectron spectra has been described in detail earlier [16, 17] and only a brief outline is given here. Clusters were produced in a supersonic expansion of Ar through a liquid nitrogen cooled nozzle. The set-up includes a differentially pumped expansion chamber, which is separated from the main interaction chamber by a conical skimmer. The use of copper nozzles with a conical profile ensures good thermal properties and efficient condensation of the expanding gas. The mean size $\langle N \rangle$ of the clusters can be empirically related to the combination of nozzle geometry, temperature and stagnation pressure [10]. In the present data we use the designation $\langle N_{sc} \rangle$ to refer to mean cluster sizes determined in this way. Photoelectrons produced by interaction of the synchrotron radiation with the cluster jet were detected in a hemispherical electron analyzer (Scienta ES 200) mounted in the dipole plane under the 'magic angle' of 54.7° to the horizontal. Within the dipole approximation, differential cross sections measured in this geometry are proportional to the total cross sections for the respective processes. Spectra of large Ar clusters ($\langle N_{sc} \rangle$ = 1670) were recorded with a pass energy of 5 eV and an approx. total apparatus energy resolution of 20 meV. The transmission function of the analyser was determined from the area of the atomic Ar $3p_{1/2}$ photoelectron line, normalized to the atomic 3p cross section and the beamline flux as measured with a GaAs photodiode of known quantum efficiency (see [9]). Spectra shown vs. binding energy were calibrated to the known ionization energies of the atomic 3p levels, i.e. 15.760 and 15.937 eV [18].

Further information on the structure of the spectrum for very low kinetic energies, and on the cluster size dependence, was obtained by using a newly commissioned apparatus employing a magnetic bottle electron spectrometer [19,20]. In this set-up, the cluster source described in Ref. [16] is mounted horizontally into an expansion chamber backed by a 1000 l/s turbopump. For alignment, the source is mounted on an xyz manipulator. The molecular beam is directed through a commercially available skimmer (Beam Dynamics) into the interaction zone, where it subtends an angle of 90° with the synchrotron radiation beam. Behind the interaction region, the cluster jet can be probed with a quadrupole mass spectrometer, before it is dumped into a 900 l/s Mac Mahon type cryopump. For maintenance purposes, both the expansion chamber and the cryopump can be separated from the main chamber by gate valves.

Additional 360 l/s and 240 l/s turbopumps are attached to the main chamber and the detector section of the magnetic bottle spectrometer. Electrons produced after photoionization of the clusters are directed into the drift tube of the magnetic bottle spectrometer, which is mounted vertically, pointing upwards. Further details of the spectrometer will be described elsewhere [20]. The instrument is operated in the single bunch mode of the storage ring. Times-of-flight are measured relative to the BESSY bunch clock. Experiments reported here were carried out on the TGM4 beamline, which is situated on a bending magnet. An energy resolution of $E/\Delta E \approx 20$ was obtained under these conditions.

An independent experiment was carried out to obtain a measure of the cluster size as an alternative to the determination via the scaling laws mentioned above. The inner valence or core level photoelectron spectra of noble gas clusters show that bulk and surfaces atoms have different electron binding energies, arising mainly from differences in the extent of final state polarization [21]. Normally, these can be resolved easily. Using the Scienta analyser we have therefore recorded the Ar 3s photoemission line under various expansion conditions, and have determined the bulk/surface peak intensity ratio. Assuming e.g. icosahedral clusters, this quantity can be directly related to the cluster size [4,9] (when intensity losses due to inelastic scattering are neglected). In agreement with our earlier study [9] it was found that the mean sizes derived from photoemission are larger than those from the scaling laws. The agreement is better for larger cluster sizes: For $\langle N_{sc} \rangle = 40$, 90 and 150 photoemission results in a mean size of $N_{ph} = 160$, 200 and 300, respectively, where the subscript "ph" designates "photoemission".

3. Results and discussion

The argon 3p valence region was measured with high resolution (Scienta analyser) for $\langle N_{sc} \rangle = 1670$ from the threshold up to a photon energy of 28 eV in steps of 0.2 eV. A single scan spectrum at $h\nu = 16.9$ eV as well as the complete data set in the form of a contour plot for intensity as a function of binding energy and photon energy are shown in Figure 1. For most photon energies the individual photoelectron spectra (intensity vs. binding energy) are very similar to previous results (e.g. Ref. [8], $h\upsilon = 26$ eV for $\langle N \rangle = 250$ and Fig. 1 of Ref. [22], $\langle N \rangle = 270$). The spectra consist of a largely unstructured cluster valence band of approximately 1.5 eV width on the low binding energy side of the two spin-orbit split atomic lines. In general, the valence bands of rare gas clusters are expected not only to show spin-orbit splitting, but also a further splitting of the $np_{3/2}$ level into its magnetic sub-levels $m_j = \pm 3/2$,

±1/2 due to the interaction between neighbouring atoms (sometimes referred to as crystal field splitting) [23]. Moreover, contributions from both bulk and surface atoms [3-9] are expected, with the result that the 1.5 eV-broad 3p-derived feature from Ar clusters is expected to contain altogether six component peaks. In the case of xenon, where the spin-orbit splitting is greater, this fine structure is strongly apparent and Rolles et al were able to perform a fit using six component features [8]. As they remark, however, the situation is less straightforward for krypton and argon, and their fit for the latter system requires unphysical values of the spin-orbit coupling.

In the present paper we concentrate on the narrow range of parameter space just above threshold, where the spectra contain a unique feature. Between $h\upsilon$ = 15.5 and 17.7 eV a strong peak at ≈ 15 eV binding energy with a halfwidth of about 0.25 eV superimposed on the 1.5 eV-broad cluster band is visible, as shown in Figure 1a. In fact, it not only dominates the spectrum, but also shifts smoothly and continuously by 0.7 eV in binding energy from 14.6 to 15.3 eV over this photon energy range. This dispersion-like behaviour is indicated by black dots in Figure 1b, which represent the peak maxima in the spectra in the photon energy range $h\upsilon$ = 15.5 and 17.5 eV. Concerning the spectra at $h\upsilon$ = 15.5 and 15.7 eV we must remember that the feature corresponds to a kinetic energy of less than 1 eV, for which the transmission of the analyzer is very low, which in turn makes it hard to differentiate between spectral features and noise. Note that Figure 1a also shows a feature at 15.5 eV binding energy, which occurs with varying intensity at almost all photon energies up to 28 eV. It is, however, never so intense as the dispersing feature and does not show dispersion.

Also shown schematically in Figure 1b are the corresponding photoemission data from Kassühlke et al. [13] for (111) single crystal bulk argon recorded in normal emission. They show only two features in the binding energy range 12.5 to 15.0 eV, one of which – like the feature in the cluster data – dominates the spectra between 16 and 18 eV photon energy and also shifts to higher binding energy by about 0.6 eV (dashed line marked '1'). In fact, the slope is approximately the same as the corresponding feature from the cluster, although the latter is not as straight; the two lines are separated by about 0.5 eV in binding energy. The other, weaker feature in the data of Kassühlke et al. (dashed line '2') shifts slightly to lower binding energy with the slope increasing at about 18 eV photon energy. The band shifts to a binding energy of about 12.6 eV at $h\upsilon$ = 23 eV. The total bandwidth is thus about 1.5 eV. There is no obvious counterpart to this band in the cluster spectra, although the contour plot does show

regions of higher intensity at a binding energy of 14.5 eV for some photon energies. Significantly, the strong feature (line '1') is also clearly present in the early photoemission data of Schwentner et al. [12], whose argon samples were not ordered. Unfortunately, there are probably very few examples in the literature of dispersion being observed in poly-crystalline systems. In fact, apart from the case of krypton in the same paper of Schwentner et al [12], we have not been able to find any! This is no doubt due to the fact that even in the early days of photoemission at variable photon energy, single crystal samples were available. The elucidation of electronic band structure was the main object, for which carefully prepared metal and semiconductor single crystals surfaces were obviously preferred.

We note the identical photon energy range, the very similar binding energy shift and the high intensity of the ≈ 15 eV feature in the single crystal, polycrystalline film and cluster data (in all three cases the feature dominates the spectra). We therefore conclude that the same effect is occurring in the cluster as in the bulk and may be attributed to energy band dispersion. In other words, there is direct evidence that at $\langle N_{sc} \rangle = 1670$ the clusters have bulk-like electronic properties. The observation of this band in photoemission for a system that is not an oriented single crystal is discussed below.

In order to determine the onset of the effect, data analogous to Figure 1 were recorded at lower resolution using the magnetic bottle analyzer for $\langle N_{sc} \rangle = 24$, 41, 96 and 191. The results are shown in Figure 2 as colour-coded intensity plots. The atomic lines in this representation appear as vertical, intense features at the right hand side of the respective panels. The increase in their apparent width towards higher photon energies results from the kinetic energy dependence of the analyser resolution; the slight changes in their position on the horizontal axis is from the combined uncertainty in the photon energy step of the monochromator and in the time-to-energy conversion. The series of sharp, intense maxima at photon energies between 15 and 16.5 eV results from second order diffraction radiation. As the time-of-flight (TOF) is measured relative to the bunch clock, only flight times up to ~800 ns (the single-bunch revolution time) can be separated. Any electron line with a TOF exceeding this value will be mapped into the spectrum resulting from the next electron bunch. Therefore, at the particular energies where the artifact is visible the TOFs of first order features overlap with the TOF of the second order outer valence line excited by the following bunch. The time-to-energy conversion, which is carried out for the time-to-energy relation of the first order lines, then leads to the erroneous appearance of the second order 3p line at similar binding energies

as the first order structure. The second order line is sharp and not resolved into cluster and atomic components due to its high kinetic energy. The same artifacts can be seen in the lower three panels of Figure 3.

The two lowest cluster sizes in Figure 2 give rise to plots resembling Figure 1b, but with a substantially reduced energy shift of the ≈ 15 eV feature. Moreover, it is less intense relative to the background from the cluster valence band. At $\langle N_{sc} \rangle = 96$ and 191 the shift approaches the value of 0.7 eV shown in Figure 1 for $\langle N_{sc} \rangle = 1670$. In particular, for $\langle N_{sc} \rangle = 191$ the data resemble closely those of Figure 1, in that the peak-to-background intensity ratio and the slope photon energy/binding energy match closely the data for the larger cluster size. This effect of mean cluster size on the observed peak shift is also demonstrated in Figure 3, which shows individual photoelectron spectra from these low resolution data sets. The lowest and highest photon energy, for which the dispersing feature at ≈15 eV binding energy (see text) is visible, are shown in each case. Arrows indicate the actual binding energy of the feature at the respective photon energy. Clearly, the range over which dispersion can be observed increases with increasing mean cluster size. Figure 3 also shows that, as a function of mean cluster size, the overall width of the 3p valence band increases from about 1.25 eV for $\langle N_{sc} \rangle = 24$ to about 1.5 eV for $\langle N_{sc} \rangle = 191$. In the photoemission spectra of bulk, polycrystalline argon the width of the valence band emission is about 1.8 eV [12].

We conclude from Figures 2 and 3 that the dispersion effect is fully developed for a mean cluster size of $\langle N_{sc} \rangle = 200$, and that the threshold is approximately at $\langle N_{sc} \rangle = 100$. These correspond to values of about $N_{ph} = 400$ and 230, respectively, according to the determination of average cluster size via photoemission. We suggest that the similar, but much weaker dispersion effect observed at even smaller values of $\langle N_{sc} \rangle$ is due to the presence of larger clusters resulting from the broad size distribution.

Can our data be compared with theory? Contrary perhaps to popular belief, the electronic structure of rare gas aggregates is not easy to calculate. The problem arises in the correct description of the van der Waals interaction which provides the necessary cohesive energy in the system concerned (cluster or bulk). Conventional bonding involving valence electrons is net repulsive. Only some 40 years after the first band structure calculations has an argon band structure been recently published by Galamic-Mulaomerovic and Patterson [24], which seems to reproduce quantitatively some of the experimental data for the bulk: single particle

excitation energies, valence band width and electron affinity. We are not aware of any cluster calculations, which would also be appropriate for comparison with the present data. However, since one of the main conclusions of this work concerns the establishment of bulk electronic properties, it is useful to look at this band structure calculation and, because of the similarity of some of the data to our own, also at the single crystal results of Kassühlke et al. [13]. As described above, some of the normal emission data of Kassühlke et al. [13] for (111) single crystal films have been included in Figure 1 (dashed lines marked '1' and '2'). We tentatively assign the band ('1') to the 3p-derived band along $\Gamma_{15} - L_2$, although the extent of the measured dispersion (≈ 0.6 eV) is not as large as the bandwidth (1.83 eV) in the calculation of Ref. [24]. Similarly, the feature shown schematically by the dashed line '2' may be due the 3p-derived $\Gamma_{15} - L_3$ band. Thus, our interpretation of the bands '1' and '2' from the single crystal data [13] locates the Γ_{15} point (corresponding to the top of the valence band) at about 14 eV binding energy, consistent with the literature value of 13.8 eV. The high intensity of band '1', in particular between 16 and 18 eV, where it dominates the spectrum, is probably a result of strong optical absorption due to inter-band transitions. The electron energy loss spectrum of solid argon also shows a prominent feature in this spectral region [25].

Why is dispersion observed in the photoemission spectrum of a polycrystalline film [12], as well as in the present cluster data? A polycrystalline film consists of small, randomly oriented single crystal regions. If the clusters can be described as very small crystallites with an fcc, or near-fcc structure [26], the cluster beam experiment represents a similar situation. One possibility is that the extent of the dispersion of the 3p band along ΓL and its lack of hybridization with other bands is very similar to that along ΓX, and probably to other directions of the Brillouin zone, leading to almost isotropic emission, providing that appropriate final state bands are available. (See Ref. [11], chapter 7.) A glance at the band structure indicates that the latter may not necessarily be the case. Alternatively, and probably more likely, the transition is restricted to a narrow range of directions in the Brillouin zone. Those clusters with approximately the correct orientation for observing emission from that particular direction, or directions, will produce the effect, particularly if the matrix element is large.

Despite the uncertainties associated with the broad cluster size distribution and the determination of mean cluster size, the present data show that the threshold for the observation of a dispersion effect occurs at cluster sizes $N_{ph} \approx 230$. If the clusters were to have

the near-fcc, icosahedral structure this number of atoms corresponds to a structure containing three and four shells. We will now rationalize this "early" transmission from molecular to bulk-like properties by recalling some general ideas of electronic structure at a text-book level e.g. [27]. Let us assume the presence of small crystallites with a bulk fcc structure and a diameter of about six or seven atoms, corresponding to just over three complete shells. If we consider the bonding of, say, the $3p_x$ orbitals in a one-dimensional row of seven argon atoms, then in an LCAO, or simple tight binding model, seven discrete levels would be created. The separation between the most bonding molecular orbital and the most anti-bonding molecular orbital we identify with the measured dispersion of about 0.7 eV. The observation of a smooth continuous shift of the strong ≈ 15 eV feature in the present experiment then implies that the intrinsic broadening mechanisms (and/or the instrumental resolution) give rise to an observed linewidth that is greater than the mean separation between the discrete levels. Continuing in this simple picture, the separation is expected to be approximately 0.1 eV, but already smeared out because of the cluster size distribution and the effect of three dimensions. On the other hand, the linewidth of the ≈ 15 eV feature is about 0.25 eV, i.e. considerably higher than that due to any remaining discrete levels. Instrumental linewidth clearly does not play a role, since there is essentially no difference between the high and low resolution data sets.

4. Summary and conclusions

In photoemission investigations of argon clusters in a free molecular beam we have observed a strong feature in the valence band region, the binding energy of which changes continuously with the photon energy. The feature is sharp with a fwhm of approx. 0.25 eV and shifts in binding energy by 0.7 eV over the photon energy range 15.5 to 17.7 eV. It is unique in the photoemission spectrum being found only in a very small region of parameter space (we have measured up to 28 eV photon energy). The photon-energy dependent binding energy shift is dependent on cluster size: the threshold for its observation appears to be at about a (scaling law) mean cluster size of $\langle N_{sc} \rangle = 100$ and it reaches its full extent of 0.7 eV after about $\langle N_{sc} \rangle = 200$ atoms has been reached. A very similar feature has been observed in almost exactly the same photon energy and binding energy ranges for both polycrystalline argon films and (111)-oriented argon single crystals. We assign it to energy band dispersion. Its appearance at this (surprisingly low) mean cluster size is an indication of the onset of bulk properties. The observation of dispersion despite the lack of preferred orientation of the clusters is also unexpected, but is explicable within the framework of the conventional photoemission model.

Acknowledgements: We thank P. Feulner, K. Horn, D. Menzel, A. Nilsson, M. Scheffler, A. Stampfl and G. P. Williams for useful discussions. Moreover, we acknowledge financial support from the Deutsche Forschungsgemeinschaft, the Advanced Study Group of the Max-Planck-Society, the Fonds der chemischen Industrie, the Swedish Research Council (VR), and the Seventh Framework Programme of the European Community (FP7/2007-2013; grant agreement no. 226716).

References

⊕: Present address: Fritz-Haber-Institut der Max-Planck-Gesellschaft, Faradayweg 4- 6, 14195 Berlin, Germany.

*: Present address: MAX-lab, Lund University, P.O. Box 118, SE-22100 Lund, Sweden.

+: Mail address: c/o Helmholtz-Zentrum Berlin, Albert-Einstein-Str. 15, 12489 Berlin, Germany. E-Mail: uwe.hergenhahn@ipp.mpg.de

1. J. Stapelfeldt, J. Wörmer, and T. Möller, Phys. Rev. Lett. **62**, 98 (1989).

2. J. Wörmer, M. Joppien, G. Zimmerer, and T. Möller, Phys. Rev. Lett. **67**, 2053 (1991).

3. U. Hergenhahn, A. Kolmakov, M. Riedler, A. R. B. de Castro, O. Löfken, and T. Möller, Chem. Phys. Lett. **351**, 235 (2002).

4. M. Tchaplyguine, R. R. Marinho, M. Gisselbrecht, J. Schulz, N. Mårtensson, S. L. Sorensen, A. Naves de Brito, R. Feifel, G. Öhrwall, M. Lundwall, S. Svensson, and O. Björneholm, J. Chem. Phys. **120**, 345 (2004).

5. R. Feifel, M. Tchaplyguine, G. Öhrwall, M. Salonen, M. Lundwall, R. R. T. Marinho, M. Gisselbrecht, S. L. Sorensen, A. Naves de Brito, L. Karlsson, N. Mårtensson, S. Svensson, and O. Björneholm, Eur. Phys. J. D **30,** 343 (2004).

6. T. Hatsui, H. Setoyama, N. Kosugi, B. Wassermann, I. L. Bradeanu, and E. Rühl, J. Chem. Phys. **123**, 154304 (2005).

7. D. Rolles, H. Zhang, Z. D. Pesic, R. C. Bilodeau, A. Wils, E. Kukk, B. S. Rude, G. D. Ackermann, J. D. Bozek, R. Diez Muiño, F. J. Garcia de Abajo and N. Berrah, Phys. Rev A **75**, 031201 (2007).

8. D. Rolles, H. Zhang, Z. D. Pesic, J. D. Bozek, and N. Berrah, Chem. Phys. Lett. **468**, 148 (2009).

9. U. Hergenhahn, S. Barth, V. Ulrich, M. Mucke, S. Joshi, T. Lischke, A. Lindblad, T. Rander, G. Öhrwall, and O. Björneholm, Phys. Rev. B **79**, 155448 (2009).

10. O. F. Hagena, Rev. Sci. Instrum. **63**, 2374 (1992).
11. S. Hüfner, *Photoelectron Spectroscopy, 3rd edition*, Springer-Verlag, Berlin 2003.
12. N. Schwentner, F.-J. Himpsel, V. Saile, M. Skibowski, W. Steinmann, and E. E. Koch, Phys. Rev Lett. **34**, 528 (1975).
13. B. Kassühlke, P. Feulner, and D. Menzel, private communication. See B. Kassühlke, PhD Thesis, Technical University of Munich (1999), Herbert Utz Verlag, Munich (1998).
14. M. Förstel, M. Mucke, T. Arion, T.Lischke, S. Barth, V. Ulrich, G. Öhrwall, O. Björneholm, U. Hergenhahn and A. M. Bradshaw, Phys. Rev. B, doi: 10.1103/PhysRevB.82.125450.
15. R. Follath and J. S. Schmidt, in *Synchrotron Radiation Instrumentation: Eighth International Conference*, edited by T. Warwick, J. Arthur, H. A. Padmore and J. Stöhr (American Institute of Physics, San Francisco, 2003), AIP Conference Proceedings Vol. 705, p. 631-634.
16. S. P. Marburger, O. Kugeler, and U. Hergenhahn, in *Synchrotron Radiation Instrumentation: Eighth International Conference*, edited by T. Warwick, J. Arthur, H. A. Padmore and J. Stöhr (AIP, San Francisco, 2003), AIP Conference Proceedings Vol. 705, p. 1114.
17. S. Barth, S. Joshi, S. Marburger, V. Ulrich, A. Lindblad, G. Öhrwall, O. Björneholm, U. Hergenhahn, J. Chem. Phys. 122 (2005) 241102.
18. I. Velchev, W. Hogervorst, and W. Ubachs, J. Phys. B **32**, L511 (1999).
19. P. Kruit and F. H. Read, J. Phys E: Sci. Instrum. **16**, 313 (1983).
20. M. Mucke *et al*., to be published.
21. O. Björneholm, F. Federmann, F. Fössing, T. Möller, P. Stampfli, J. Chem. Phys. 104 (1996) 1846.
22. H. Zhang, D. Rolles, J.D. Bozek, N. Berrah, J. Phys. B 42 (2009) 105103.
23. K. Horn, M. Scheffler, and A. M. Bradshaw, Phys. Rev Lett. **41**, 822 (1978).
24. S. Galamic-Mulaomerovic and C. H. Patterson, Phys. Rev. B **71**, 195103 (2005).
25. L. Schmidt, Phys. Lett. **36A**, 87 (1971).
26. S. Kakar, O. Björneholm, J.Weigelt, A. R. B. de Castro, L. Tröger, R. Frahm, T. Möller, A. Knop, and E. Rühl, Phys. Rev. Lett. **78**, 1675 (1997).
27. A. M. Bradshaw and M. Scheffler, J. Vac. Sci. Tech. **16**, 447 (1979).

Figure captions

FIG. 1. (Color online) a. Single scan high resolution 3p photoelectron spectrum of Ar clusters with mean size $\langle N_{sc} \rangle = 1670$ at $h\nu = 16.9$ eV (Scienta analyser) showing the ≈ 15 eV feature. b. Contour plot of the complete data set as a function of both photon energy and binding energy. The black dots represent the intensity maxima of the ≈ 15 eV feature showing strong energy band dispersion. The lines designated '1' and '2' represent dispersing features in the photoemission data for Ar(111) measured by Kassühlke et al [13]. The feature '2' extends to lower binding energies, but is not plotted here.

FIG. 2. (Color online) Colour coded intensity plots of 3p photoelectron spectra of Ar clusters with various mean sizes of $\langle N_{sc} \rangle = 24$ (panel a), $\langle N_{sc} \rangle = 42$ (b), $\langle N_{sc} \rangle = 96$ (c) and $\langle N_{sc} \rangle = 191$ (d). These are low resolution data recorded with the magnetic bottle spectrometer. The sharp, intense features below $h\upsilon = 16.7$ eV are due to second order radiation from the mono-chromator (see text).

FIG. 3. (Color online) Low resolution 3p (valence band) photoelectron spectra of Ar clusters for different mean cluster sizes recorded with the magnetic bottle analyser. In each case, the lowest and highest photon energy, for which the dispersing feature at ≈15 eV binding energy (see text) is visible, are shown. Arrows mark the respective binding energy values, and demonstrate that the range over which dispersion can be observed increases with increasing mean cluster size. At the same time, the valence band width increases, as seen from the low energy cut-off. The very sharp peak is a second order feature from the monochromator (see text).

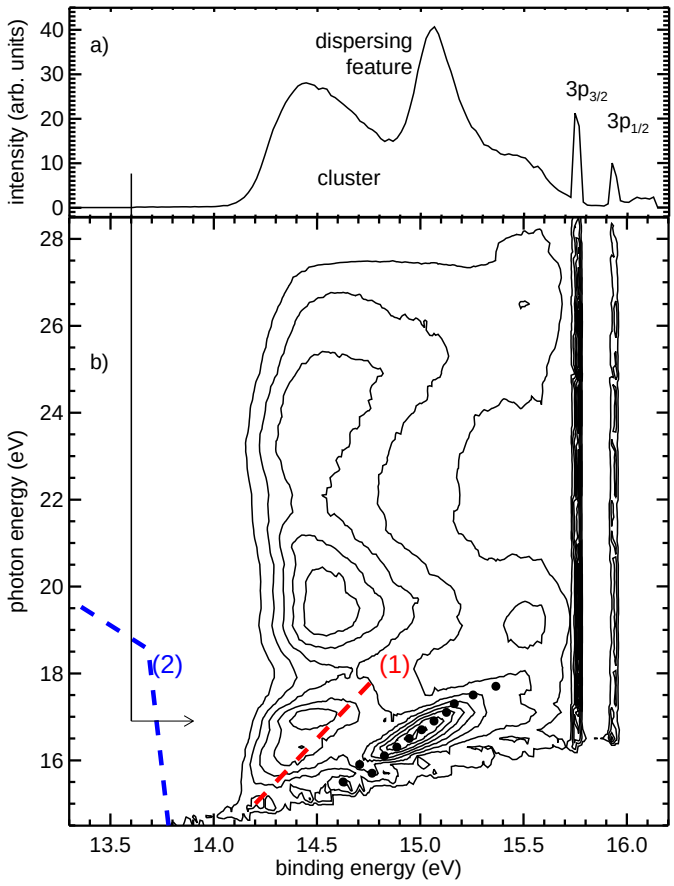
a)
dispersing
feature
3p3/2
3p1/2
cluster
intensity (arb. units)
40
30
20
10
0
b)
(1)
(2)
photon energy (eV)
28
26
24
22
20
18
16
13.5
14.0
14.5
15.0
15.5
16.0
binding energy (eV)

Figure 1

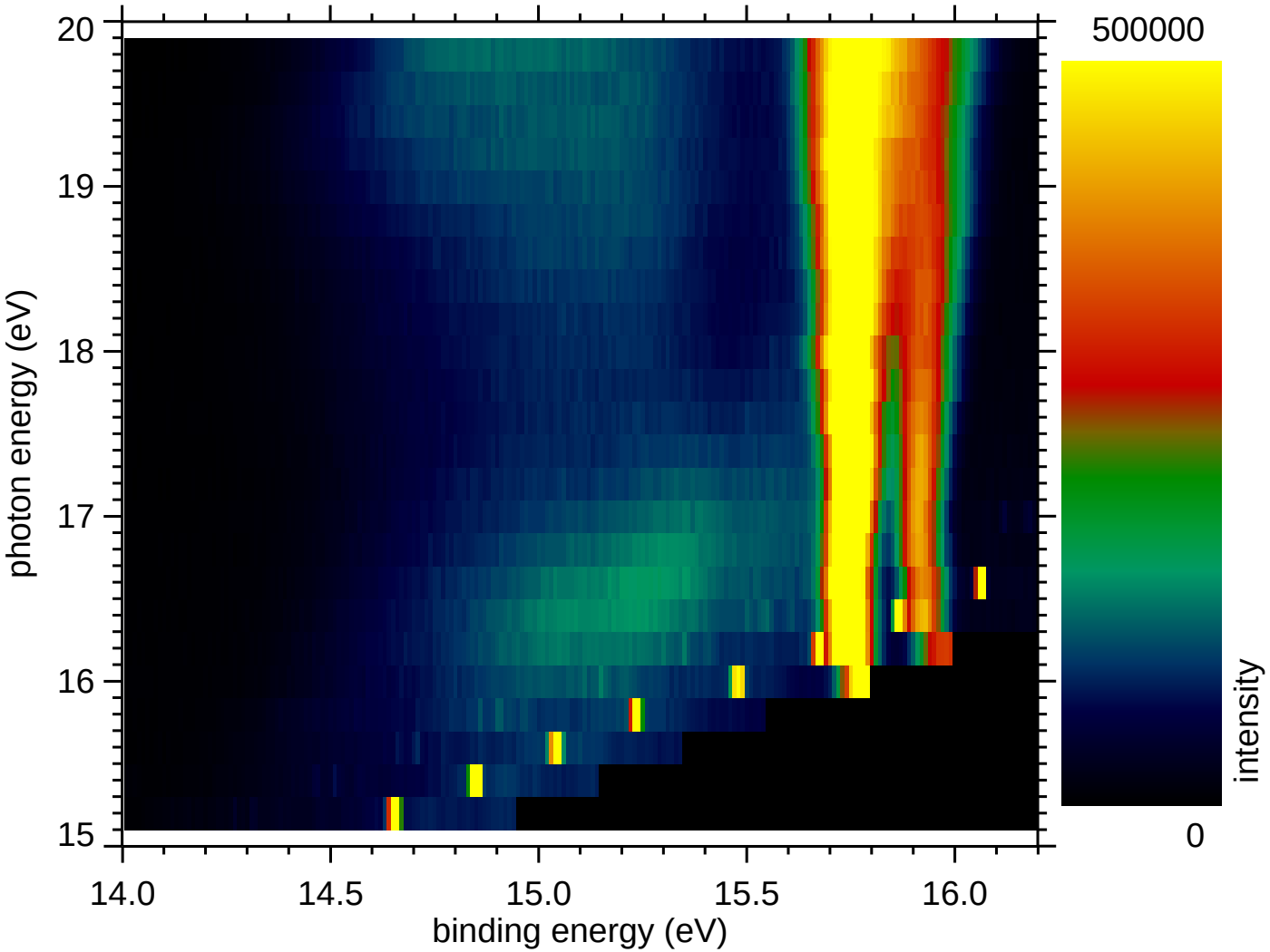
a) <N_sc> = 24
20
19
18
17
16
15
photon energy (eV)
14.0
14.5
15.0
15.5
16.0
binding energy (eV)
500000
0
intensity

Figure 2

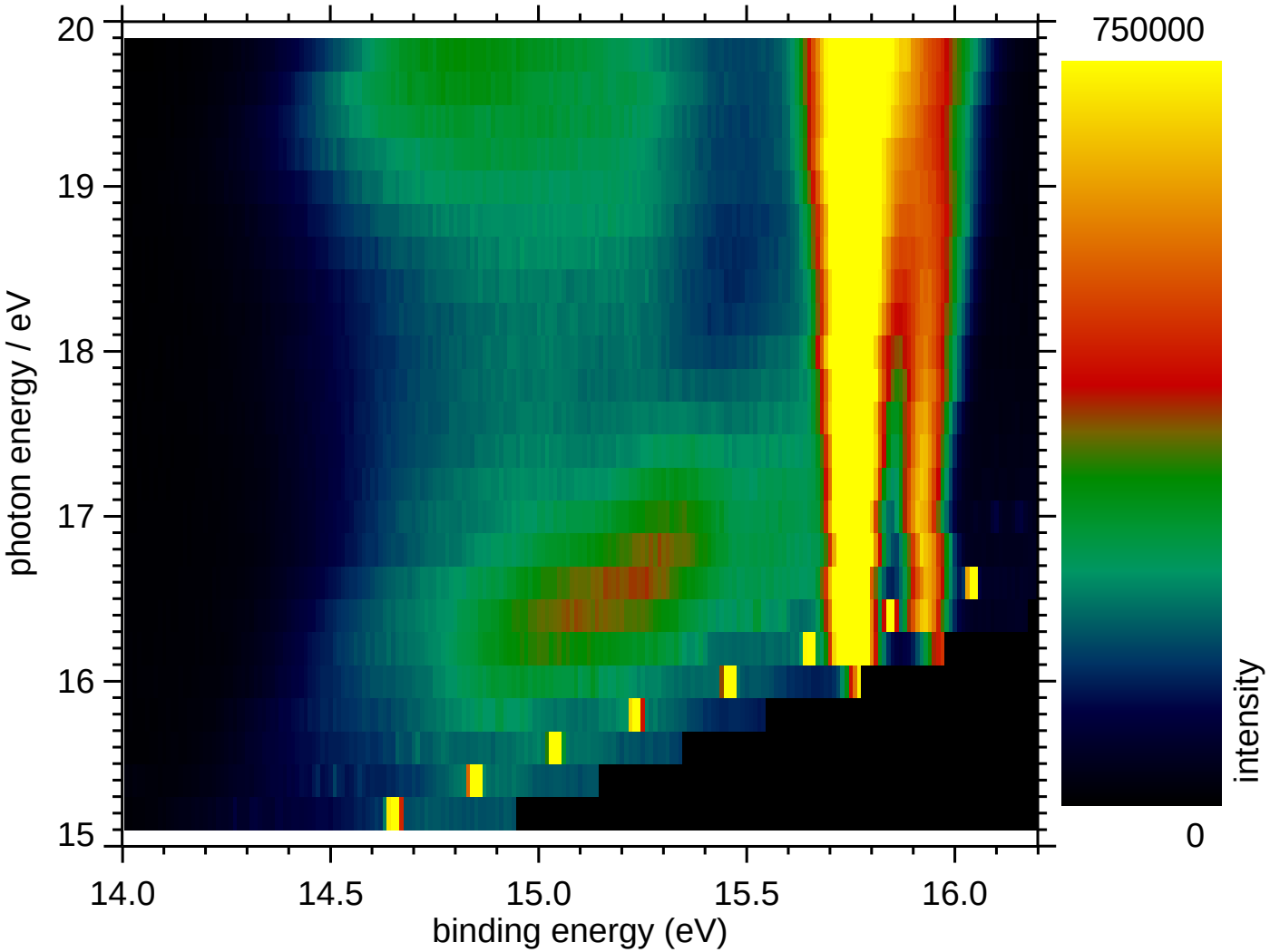
b) <N_sc> = 42
20
19
18
17
16
15
photon energy / eV
14.0
14.5
15.0
15.5
16.0
binding energy (eV)
750000
0
intensity

Figure 2

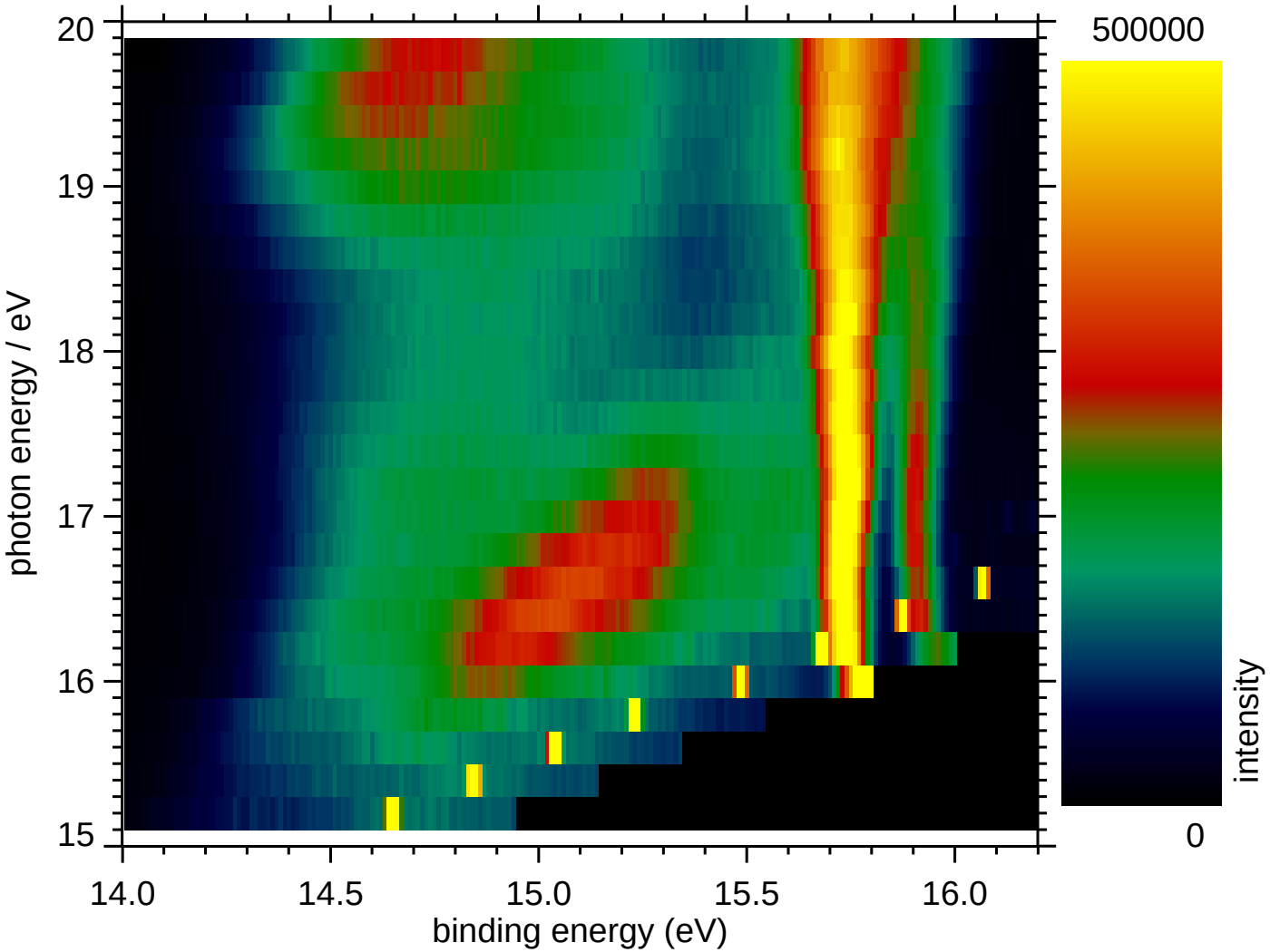
c) <N_sc> = 96
20
19
18
17
16
15
photon energy / eV
14.0
14.5
15.0
15.5
16.0
binding energy (eV)
500000
0
intensity

Figure 2

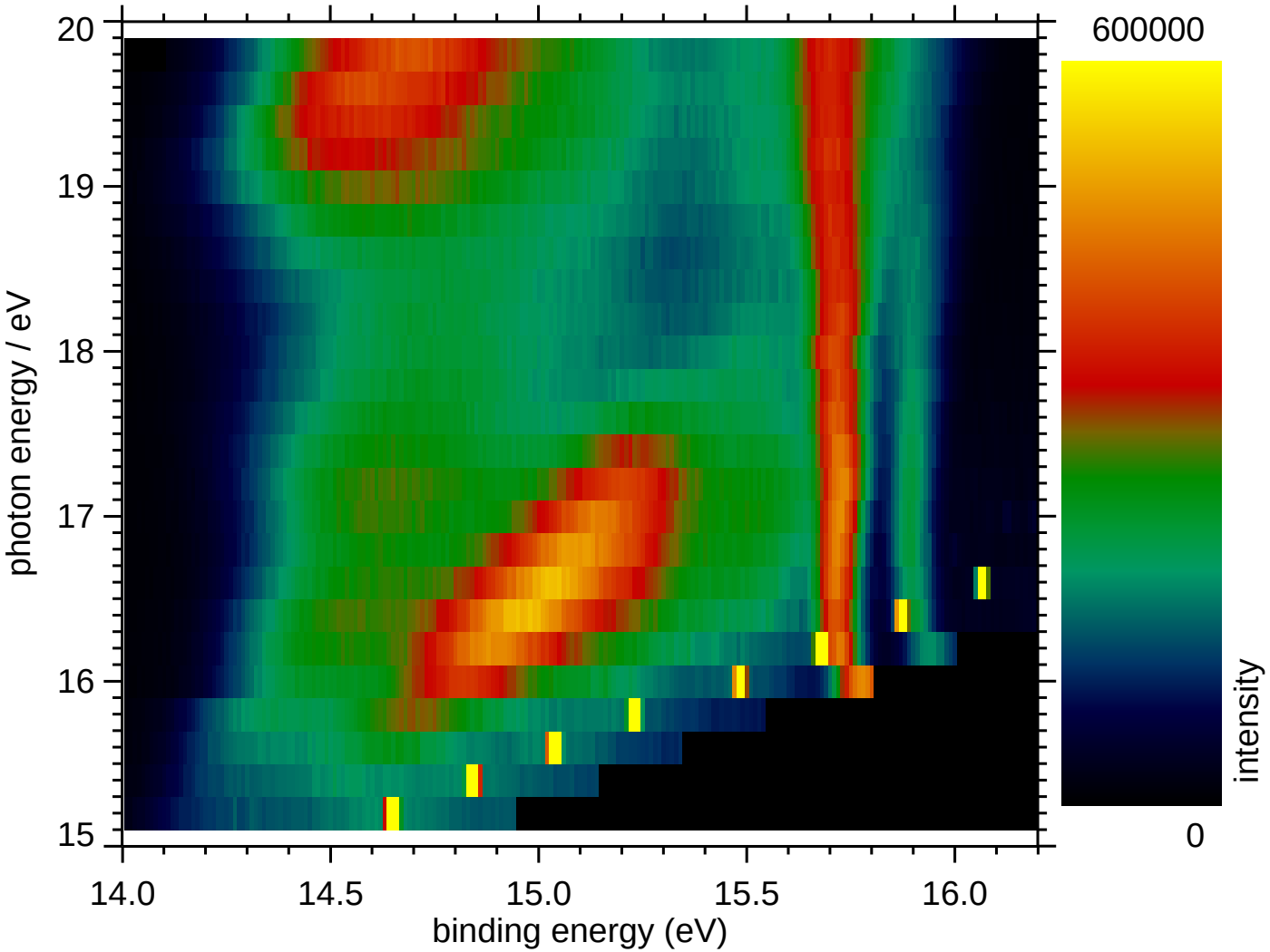
d) <N_sc> = 191
20
19
18
17
16
15
photon energy / eV
14.0
14.5
15.0
15.5
16.0
binding energy (eV)
600000
0
intensity

Figure 2

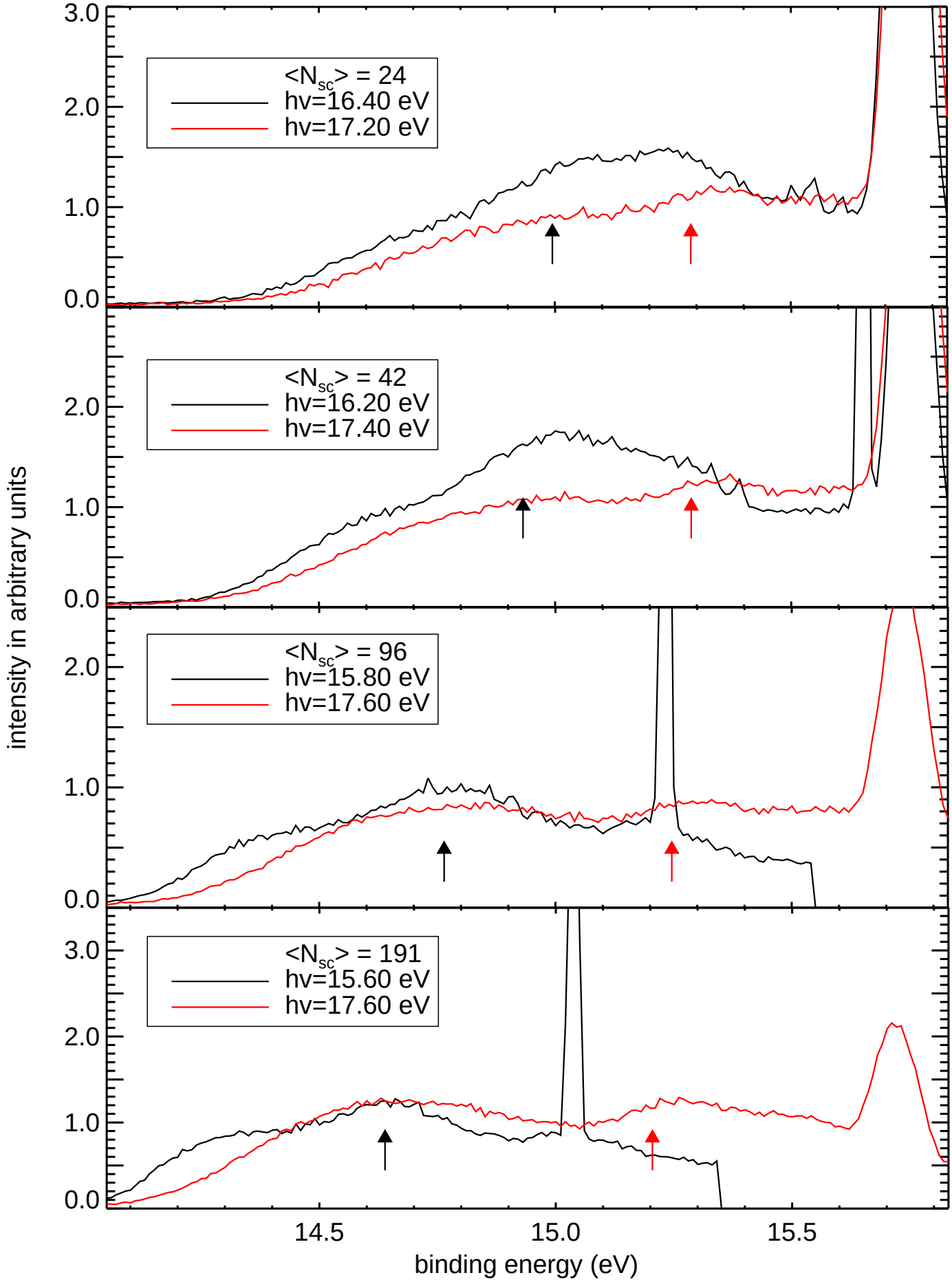
<N_sc> = 24
hv=16.40 eV
hv=17.20 eV
<N_sc> = 42
hv=16.20 eV
hv=17.40 eV
<N_sc> = 96
hv=15.80 eV
hv=17.60 eV
<N_sc> = 191
hv=15.60 eV
hv=17.60 eV
intensity in arbitrary units
binding energy (eV)
0.0
1.0
2.0
3.0
14.5
15.0
15.5

Figure 3